Exoplanet Characterisation Observatory (EChO)

Assessment Phase Payload Study

Noise Budget

ECHO-TN-0002-RAL

Issue 2.4

Prepared by: E. Pascale and I. Waldmann Date:

Checked / Approved by: Digitally signed by Paul Eccleston Date: 2013.11.29 15:24:11 Z Date:

DOCUMENT CHANGE DETAILS

Issue	Date	Page	Description Of Change	Comment

DISTRIBUTION LIST

EChO Payload Consortium				External	
Co-PIs / Science Team Coordinators		Study Engineering Team Working Group Leads		European Space Agency	
✓	Giovanna Tinetti	✓	Paul Eccleston		Philippe Escoubet
	Hans Ulrik Nørgaard-Nielsen		Ranah Irshad		Ana Heras
	Jean-Philippe Beaulieu		Emanule Pace		Didier Martin
	Paul Hartogh		Gianluca Morgante		Kate Isaak
	Giusi Micela		Berend Winter		Ludovic Puig
	Ignasi Ribas		Marc Ferlet		Martin Linder
	Bruce Swinyard		Mercedes Lopez-Morales		Nicola Rando
	Mark Swain		Vince Coudé du Foresto		
	Tanya Lim		Alberto Adriani		
	Neil Bowles		Jean-Michel Reess		
	Enzo Pascale		Marc Ollivier		
	Gillian Wright		Gonzalo Ramos Zapata		
	Graziella Branduardi-Raymont		Neil Bowles		
	Marc Ollivier	**Other Engineering Team**			
	Pierre-Olivier Lagage		*As necessary for doc*		
	Vince Coudé du Foresto				
	Athena Coustenis				
	Emanuele Pace				
	Giuseppe Piccioini				
	Giuseppe Malaguti				
	Alessando Sozzetti				
	Maria Rosa Zapataro Osorio				
	Mercedes Lopez-Morales				
	Enric Palle				
	Christopher Jarchow				
	Denis Grodent				
	Allan Hornstrup				
	Geza Kovacs				
	Pierre Drossart				
	T Encrenaz				
	L Fletcher				
	D Pinfield				
	J Cho				
	F Forget				
	I Waldmann				
	P Deroo				
	I Mueller-Wodarg				
	F Selsis				
	O Grasset				
	L Stixrude				
	T Guillot				
	Others…				

TABLE OF CONTENTS

1 OVERVIEW

1.1 SCOPE

This document describes the noise sources, which will affect spectroscopic observations made by the EChO instrument. A detailed breakdown is presented quantifying the contribution that each noise component has to the total noise budget.

1.2 APPLICABLE DOCUMENTS

AD #	APPLICABLE DOCUMENT TITLE	DOCUMENT ID	ISSUE / DATE
1	EChO Mission Requirements Document (MRD)	**SRE-PA/2011.038/**	Iss. 3 – 14/09/12
2	EChO Science Requirement Document (SciRD)	**SRE-PA/2011.037**	Iss. 0.1 – 24/05/13
3			

1.3 REFERENCE DOCUMENTS

RD #	REFERENCE DOCUMENT TITLE	DOCUMENT ID	ISSUE / DATE
1	EChOSim Software Requirements Document (EChOSim SRD)	**ECHO-TN-0002-CF-SRD**	2.0
2	EChOSim User Requirements Document (URD)	**ECHO-TN-0001-CF-URD**	3.0
3	Pointing Jitter Impact on Photometric Stability	**ECHO-TN-0003-UCL**	
4	EChO Assessment Study Design Report	**ECHO-RP-0001-RAL**	1.5
5	Comparison between EChOSim 3.0 and ESA Radiometric model	**ECHO-TN-0001-UCL**	0.8
6	Radiometric Background Modeling for the EChO Payload Instrument	**ECHO-TN-0006-UCL**	0.2

2 INTRODUCTION

The goal of this document is to quantify the noise budget for the EChO instrument baseline design described in RD4. The design comprises a telescope feeding 4 spectroscopic channels arranged into modules on a common optical bench. The instrument design is required to provide continuous wavelength coverage from 0.55 to 11µm (R-PERF-150, AD1) and covers 0.4 to 16µm as a goal (G-PERF-16, AD1). The four EChO channels and their respective wavelength coverage are (RD4):

- VNIR: from 0.4µm to 2.47µm;
- SWIR: from 2.47µm to 5.3µm;
- MWIR: from 5.3µm to 11.25µm;
- LWIR: from 11.25µm to 16µm.

A detailed breakdown of each noise source affecting the measurement in each of these wave bands is provided here. The contribution of each noise component is compared against the requirements given in R-PERF-350 of the MRD. This is done for two limiting target cases:

i) The faintest star to be observed by the EChO payload given by R-PERF-090 corresponding to the target GJ1214;

ii) The brightest star to be observed by the EChO payload given by R-PERF-110, corresponding to the target 55 Cnc.

The box below summarises, for convenience, the relevant requirements.

==========

R-PERF-090 The faintest star to be observed by the EChO payload shall be defined as follows:

	Type	K magnitude	Comment
Under 3 microns	M5V	8.8	GJ 1214
From 3 to 8 microns	G0V	9.0	
Above 8 microns	G0V	8.0	

The flux from these targets can be evaluated using the appropriate SED from the library provided, and are based on the following parameters:

	T [K]	Radius [r_{Sun}]	Distance [pc]
Under 3 microns	3200	0.19	13
From 3 to 8 microns	6030	1.05	150
Above 5 microns	6030	1.05	94.6

R-PERF-110 The brightest star to be observed by the EChO payload shall be defined as follows:

	Type	K magnitude	Comment
All wavelengths	K0V	4.0	55 Cnc

The flux from this target can be evaluated using the appropriate SED from the library provided, and are based on the following parameters:

	T [K]	Radius [r_{Sun}]	Distance [pc]
All wavelengths	5250	0.80	12.3

R-PERF-350 The system level noise (after post-processing) shall be lower than X times the astronomical noise floor (defined by the square sum of the stellar and zodiacal background shot noises). The total noise $Noise_{TOTAL}$ shall then be less than:

$$\begin{aligned} Noise_{TOTAL} &\le \sqrt{(N_0 + zodi) \times (1 + X)} \\ &= \sqrt{(N_0 + zodi) + X \times (N_0 + zodi)} \\ &= \sqrt{N_0 + zodi} + (\sqrt{1 + X} - 1) \times \sqrt{(N_0 + zodi)} \end{aligned}$$

Where:

- N0 is the flux from the target star being observed.
- The zodiacal background contribution shall be evaluated using a worst case FoV per spectral bin of 10"x10" (TBC) and the average zodi value as defined in R-PERF-390.

X shall be equal to:

- 200% (TBC) under 1 micron.
- 30% between 1 and 5 micron.
- 30% above 5 micron.

==========

2.1 NOISE SOURCES

In this study we have considered the following noise sources:

Table 1: Instrument and Astrophysical Noise Sources

Noise Type	Noise Source
Detector Noise	• Detector Dark Current Noise • Detector Readout Noise
Thermal Noise	• Emission from telescope , common optics and dichroics • Emission from module enclosures
Astronomical Noise	• Photon noise arising from the target • Photon noise arising from local zodi emission
Pointing Jtter	• RPE and PRE effects on the position and shape of the detector sampled PSF

Table 1: **Noise sources**

Note1: Pointing jitter noise is a noise source which is correlated among all detector-pixels in all focal plane arrays.

Note2: For thermal noise, we consider the residual noise left after removal of the thermal background in data processing. As such, the thermal noise is considered uncorrelated because it is based on photon noise. The effect of temperature fluctuations of the optics (telescope, common optics, etc.) is assumed to be negligible (see RD4, Section 4.5) or removable in data reduction.

Note 3: Possible detector responsivity drifts are not considered in this study. It is expected that these can be controlled using an in-flight calibration strategy (see e.g. RD4).

2.2 SIMULATIONS

In this study EChOSim simulations have been used to estimate the contribution each noise source in Table 1 has to the total noise budget. EChOSim is the EChO science payload end-to-end simulator. For information about the EChOSim model of the EChO Payload, we refer to the User Definitions Document (URD, RD2). A Software Requirements Document (SRD, RD1) is also available for a detailed description of the software interfaces. EChOSim has been validated against several and different radiometric models of the EChO payload (see RD4 Section 13, and RD5).

The instrument model utilised by EChOSim is a parameterised description of the EChO payload (see Appendix for a tabulated list of parameters), and the detector focal planes use Teledyne sensors from VNIR to MWIR. The dark current and readout noise for VNIR and SWIR were provided by the manufacturer and listed in RD4 (Section 5.7, Table 5.9). For MWIR, we use the dark current derived in McMurtry et al. 2013 (SPIE, Opt. Eng. 52(9), 091804) who report that 94% of detector pixels in the array have dark current below 10 e^-/s and 92% of pixels have dark current below 1 e^-/s. Therefore we have conservatively assumed a MWIR dark current level of 100 e^-/s.

In the simulations, the instrument emission includes the emission from all optical surfaces in the line of sight of each channel detector array. We also account for the emission arising from the module's enclosures, following the implementation suggested in RD6, and accounting for the "inner-sanctum" discussed in there. See the appendix for the temperatures used in these simulations.

2.3 DATA REDUCTION

We have implemented an advanced data reduction pipeline to analyse EChOSim simulations (see RD2). The pipeline allows reducing detector timelines into calibrated spectra, and removes some of the expected systematic effects.

It is expected that the PRE component of the pointing jitter contributes to the photometric error budget. This noise component is strongly correlated among all detectors and focal planes. FGS information can be used to decorrelate this noise component from the detector timelines, hence improving the SNR of the reconstructed spectra. With this advanced data analysis technique, it has been possible to improve the SNRs of the post-processed simulations up to a factor 3.

2.4 OVERALL NOISE ALLOCATION

In the simulation, the number of detected planet + star photons, N_0, and zodi photons in sampling interval, Δt, is used to estimate the level of photon noise from the astrophysical scene. This is

$$\sigma_N^S = \sqrt{N_0 + Zodi} \quad \frac{\mathrm{e}^-}{\mathrm{pixel}} - \mathrm{rms}$$

It is convenient to refer the noise achieve in one sampling interval to the noise achievable in the unit time:

$$\sigma_N = \sigma_N^S/\sqrt{\Delta t} \quad \left[\mathrm{e}^-\mathrm{pixel}^{-1}\mathrm{s}^{-1/2} - \mathrm{rms}\right] \qquad [1]$$

All sources of instrumental noise contribute to the total system noise level, σ_{SN}. The system noise level is then given by the sum in quadrature of all individual noise components:

$$\sigma_{SN} = \sqrt{\sigma_{RO}^2 + \sigma_{DC}^2 + \sigma_{Tel}^2 + \sigma_{Opt}^2 + \sigma_{RPE+PRE}^2} \quad \left[\mathrm{e}^-\mathrm{pixel}^{-1}\mathrm{s}^{-1/2} - \mathrm{rms}\right] \qquad [2]$$

where σ_{RO} is the detector readout noise and assumes a number of non-destructive readings (NDR) following up the ramp which is target-dependent, σ_{DC} is the dark current noise, σ_{Tel} is the combined photon noise associated to the thermal emission of all optical surfaces in the line of sight, σ_{Opt} is the photon noise associated to the thermal emission of the module enclosure, and $\sigma_{RPE+PRE}$ expresses the photometric noise associated to the pointing jitter.

Figure 1 shows the results obtained for the bright target defined by R-PERF-110. The total system noise, σ_{SN}, is shown by the solid redline, and lies below the photon noise (dotted blue line) of the target, across the whole EChO required spectral band (R-PERF-150), including the EChO goal LWIR channel (G-PERF-16).

In Figure 2 we present a similar analysis for the faint target. Also in this case the system noise is smaller than the astrophysical photon noise of the target source + zodi across all EChO **required** and goal channels.

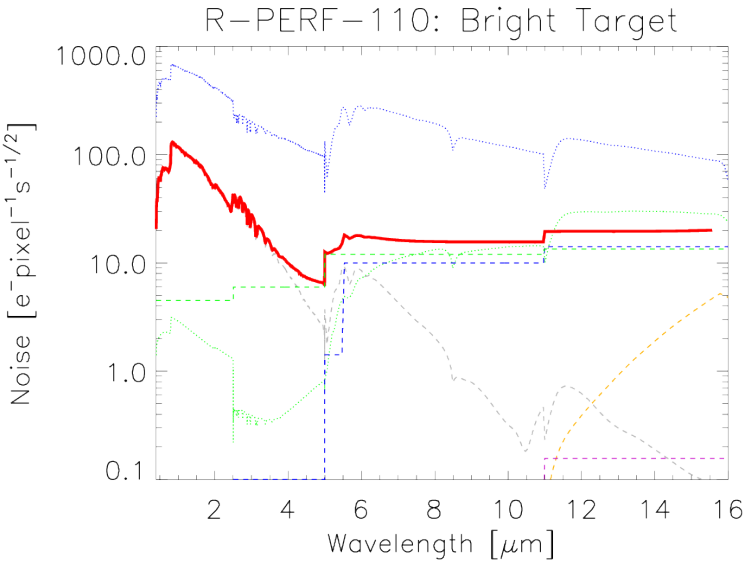

Figure 1: Noise analysis for the brightest target to be observed by EChO. Detectors are read following-up-the-ramp, with 12 non-destructive readings. The photon noise of the target and that of local zodi emission are shown by the dotted blue and green lines, respectively. The total system noise calculated using Equation 2 is shown by the red solid line. The individual noise components contributing to the system noise are estimated using EChOSim simulations, and are shown in the plot: readout noise (dashed green); dark current noise (dashed blue); thermal emission from instrument enclosures (dashed violet); thermal emission from optical surfaces (dashed yellow); post-processing RPE+PRE photometric error (dashed grey). All EChO required channels (VNIR, SWIR, MWIR) are working at the limit of the photon noise arising from astrophysical sources (star +zodi). The EChO goal LWIR channel is, also astrophysical photon-noise limited.

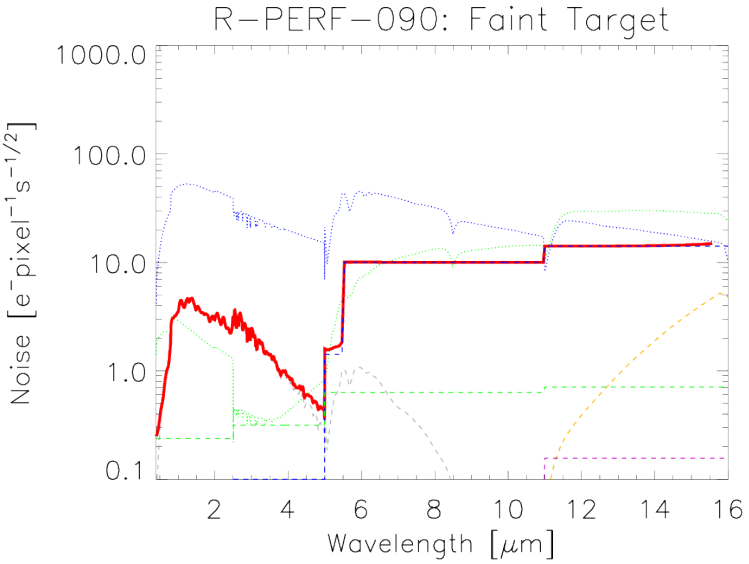

Figure 2: Noise analysis for the faintest target to be observed by EChO. Detectors are read following-up-the-ramp, with 30 non-destructive readings. The photon noise of the target and that of local zodi emission are shown by the dotted blue and green lines, respectively. The total system noise calculated using Equation 2 is shown by the red solid line. The individual noise components contributing to the system noise are estimated using EChOSim simulations, and are shown in the plot: readout noise (dashed green); dark current noise (dashed blue); thermal emission from instrument enclosures (dashed violet); thermal emission from optical surfaces (dashed yellow); post-processing RPE+PRE photometric error (dashed grey). All EChO required channels (VNIR, SWIR, MWIR) are working at the limit of the photon noise arising from astrophysical sources (star +zodi). The EChO goal LWIR channel is photon-noise limited by the instrument with no impact for the mission requirements.

2.5 OVERALL NOISE BREAKDOWN

The estimated photon noise from the astrophysical scene is used to express the requirement on the system noise. Following R-PERF-350, the requirement is

$$\sqrt{\sigma_{SN}^2 + \sigma_N^2} < \sqrt{{\sigma_{SN}^R}^2 + \sigma_N^2} = \left(\sqrt{1+X}\right)\sigma_N \quad [3]$$

where σ_{SN}^R is the maximum system noise allowed by the requirements. The parameter X is the excess noise-variance and it is set to $X = 2$ for the VNIR channel below 1µm, and $X = 0.3$ for the VNIR channel above 1µm. The SWIR, MWIR, and LWIR channels all have $X = 0.3$.

For each noise source contributing to σ_{SN}, we estimate its contribution to the excess noise-variance, X. This is obtained by squaring Equation 3:

$$\left[\sqrt{\sigma_{SN}^2 + \sigma_N^2}\right]^2 < \left[\left(\sqrt{1+X}\right)\sigma_N\right]^2 \quad [4]$$

Solving for X gives,

$$X = \left[\frac{\sigma_{SN}}{\sigma_N}\right]^2$$

We can use this to quantify the relative contribution each noise component has to the system noise. For instance, if σ_{RO} is the readout noise, its contribution to the excess noise-variance is:

$$X_{RO} = \left[\frac{\sigma_{RO}}{\sigma_N}\right]^2$$

and similarly for all other components contributing to the system noise. Since this number is independent from the integration time and spectral binning, it provides a convenient quantitative way to break down the noise budget in individual components.

Figures 3 and 4 below show the contributions to the system noise-variance. The dark solid line is the requirement, i.e. the R-PERF-350 X value. The red solid curve is the value of X achieved combining all noise sources from simulations. Requirements are met as long the red line lies below the black line. Figures 3 and 4 show that the EChO baseline design is compliant with the requirements over all required channels (VNIR+SWIR+MWIR) and goal LWIR channel. The gray shadowed areas in Figures 3 and 4 indicate channel transitions, in accordance to the no-cut-zone defined by the R-SCI-030 prescription. The allowed noise variance is exceeded only at the transition between the MWIR and LWIR channels for the faint target case (Figure 4).

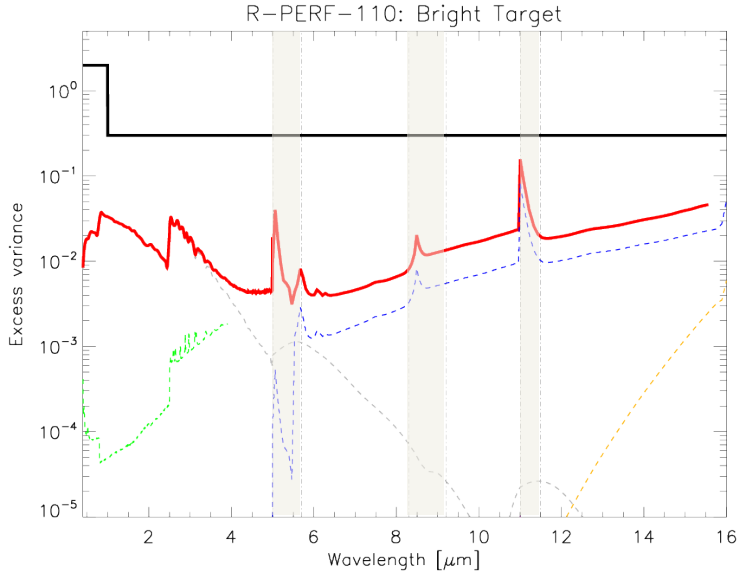

Figure 3: Noise breakdown for the brightest target to be observed by EChO. Detectors are read following-up-the-ramp, with 12 non-destructive readings. The excess variance expressed as the X-parameter defined in R-PERF-350 (see also Equations 3 and 4) is plotted on the y-axis versus wavelength. The mission requirement is displayed by the solid black line. The solid red line shows the total excess variance obtained with the EChO baseline design, which is compliant with the requirements over all required channels (VNIR+SWIR+MWIR). The individual noise components contributing to the system noise variance are estimated using EChOSim simulations, and are shown in the plot: readout excess variance (dashed green); dark current excess variance (dashed blue); thermal emission from optical surfaces excess variance (dashed yellow); post-processing RPE+PRE photometric excess variance (dashed grey).

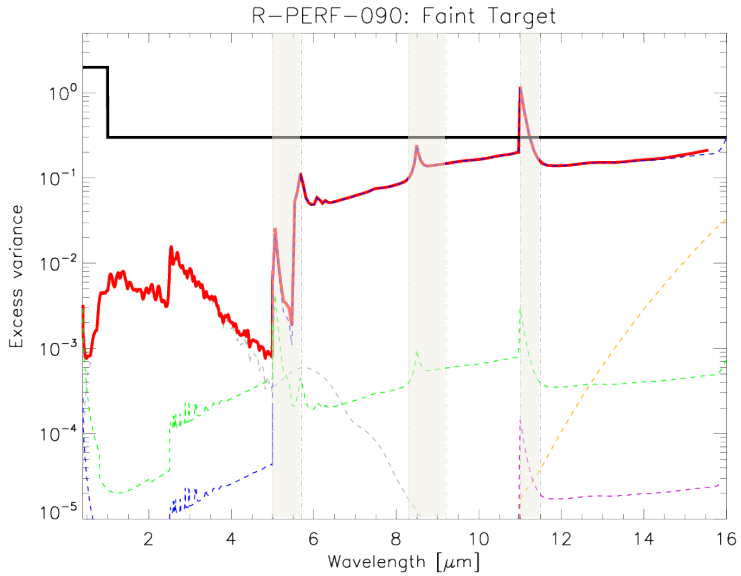

Figure 4: Noise breakdown for the faintest target to be observed by EChO. Detectors are read following-up-the-ramp, with 30 non-destructive readings. The excess variance expressed as the X-parameter defined in R-PERF-350 (see also Equations 3 and 4) is plotted on the y-axis versus wavelength. The mission requirement is displayed by the solid black line. The solid red line shows the total excess variance obtained with the EChO baseline design, which is compliant with the requirements over all required channels (VNIR+SWIR+MWIR). The individual noise components contributing to the system noise variance are estimated using EChOSim simulations, and are shown in the plot: readout excess variance (dashed green); dark current excess variance (dashed blue); thermal emission from instrument enclosures excess variance (dashed violet); thermal emission from optical surfaces excess variance (dashed yellow); post-processing RPE+PRE photometric excess variance (dashed grey).

3 CONCLUSIONS

The analysis reported here shows that the current EChO baseline design is compliant with the requirements set by R-PERF-350 and R-SCI-030 over the whole required R-PERF-150 wavelength region.

Appendix

The table below lists the parameters of the EChOSim instrument model.

	VNIR	SWIR	MWIR	LWIR
Pixel size (μm), as assumed baseline	18	18	25	25
Detector array size or used part of it	256x256	~968 max x 25	~70x13 for MWIR1 ~45x13for MWIR2	~65 x11
Slit size (" on sky)	~2" diameter(50μm fibre core)	4.1" (+0/-0.2) x 20"	6.5"(+0/-0.5) x 20"	8.3" (+0/-0.7) x 20"
Spectral resolving power R(2 pixels sampling, except VNIR)	~330, constant (order m~3-20)	~399 (TBC)at 2.45μm to ~851 at 5.45μm	~33 at 5.5μm to ~75 at 8.5μm to ~136 at 11.5μm	~50 at 11μm to ~75 at 16μm
Image plane focal ratioF#	4 (at fibre input), ~3.5 (at output), ~5.5 (at detector)	~3.1[2.0 – 4.0] average	~2.6 [1.5 – 3.5]average, ~2.1 x 3.1 in spectral-spatial	~2.0[1.5 – 2.5]
Entrance aperture A_{eff} (m^2)	1.131, telescope-defined and set at minimum ESA MRD level & consistent with ~1.455m x ~0.99m elliptical entrance pupil			
Effective focal lengthf_{eff} (m)	~4.8 (at fibre input) (i.e. ~43"/mm)	~4.39 , (i.e. ~47.0"/mm)	~3.1 (TBC), (i.e. ~66.5"/mm)	~2.4, (i.e. ~86.0"/mm)
Optical transmission (average end-to-end, excluding QE)	~0.1 [0.05 – 0.2] for λ<1.0μm, 0.3 [0.2 – 0.4] for λ>1.0μm	0.3 [0.2 – 0.4]	0.3 [0.2 – 0.4]	0.3 [0.2 – 0.4]
PSF model parameter K	Geometric image of fibre + diffraction	0.55 [0.25 – 0.85]	0.8 [0.65 – 0.95]	0.9 [0.8 – 1.0]
Ratio Kx/Ky	1 (~1.47 at fibre entrance)	~1	1.47, longer PSF spatial direction	1.47, longer PSF spatial direction

Instrument emissions have been estimated assuming a telescope and IOB at a temperature of 45K.

For the MWIR and LWIR channels, the presence of an 'inner-sanctum' at a temperature of 35K and 25K, respectively, has been assumed.

The photometric error arising from pointing RPE and PRE assume an AOCS based on cold gas (see RD3). As shown in RD3, a solution involving a reaction wheel based AOCS has no negative impact on the overall noise budget.